

## Direct and indirect methods of the plasma jet generation

A. Kasperczyk<sup>1</sup>, T. Pisarczyk<sup>1</sup>, M. Kalal<sup>2</sup>, J. Ullschmied<sup>3</sup>, E. Krousky<sup>4</sup>, K. Masek<sup>4</sup>,  
M. Pfeifer<sup>4</sup>, K. Rohlena<sup>4</sup>, J. Skala<sup>4</sup>, P. Velarde<sup>5</sup>, M. González<sup>5</sup>,  
C. Garcia<sup>5</sup>, E. Oliva<sup>5</sup>, and P. Pisarczyk<sup>6</sup>

<sup>1</sup>Institute of Plasma Physics and Laser Microfusion, 23 Hery St., 00-908 Warsaw, Poland

<sup>2</sup>Czech Technical University in Prague, FNSPE, Brehova 7, 115 19 Prague 1, Czech Republic

<sup>3</sup>Institute of Plasma Physics AS CR, v.v.i., Za Slovankou 3, 182 00 Prague 8, Czech Republic

<sup>4</sup>Institute of Physics AS CR, v.v.i., Na Slovance 2, 182 21 Prague 8, Czech Republic

<sup>5</sup>Instituto de Fusion Nuclear, Madrid, Spain

<sup>6</sup>Warsaw University of Technology, ICS, 15/19 Nowowiejska St., 00-665 Warsaw, Poland

In the paper three different methods of plasma jet generation, proposed and applied by the authors, are described. The first one is a direct method, at which a massive planar target made of a relatively heavy material (atomic number equal to, or higher than 29) was used. The two other indirect methods employed a disk impact or a cumulative compression of a conically shaped thin foil. In the former case a copper slab served as a target, whereas in the latter – a 6-9  $\mu\text{m}$  thick Al foil was used for prefabrication of disks or cones. The experiments were carried out at the Prague Asterix Laser System (PALS) iodine laser using the first and third harmonics of laser radiation with the energy in the range of 100-600 J and the pulse duration of 250 ps (FWHM). For measurement of jet parameters, such as velocity, electron density, dimensions and the like, a three-frame interferometric/shadowgraphic system was used.

### 1. Introduction

Collimated plasma outflows and jets are a subject of high interest in studying astrophysical phenomena [1, 2], as well in the simulation of the plasma jets generated at contact surfaces of different materials in a multi-shell target geometry [3, 4]. Possibilities to have such plasma jets available in laboratory conditions would allow for many original experiments to be performed. The first successful attempts to generate laboratory plasma jets relevant to astrophysical observations were described, e.g., in Refs. 5 and 6. *Conically* shaped targets made of different materials were irradiated by *five* beams of the Nova laser with pulse duration of 100 ps and energy in each beam of 225 J, or by *six* beams of the GEKKO-XII laser with the same pulse duration, but with the total energy of 500 J. In the above mentioned experiments the jet-like structures were formed by the *cumulative* effect of the ablated flows at the axis of *conical* targets.

### 2. Direct method of plasma jet generation

Recently, much simpler method of plasma jets production was proposed by the authors and developed at the Prague Asterix Laser System (PALS). It was demonstrated that a partially defocused (an interaction spot radius  $\sim 300 \mu\text{m}$ ) relatively low-energy ( $\sim 100 \text{ J}$ ) third harmonic ( $0.438 \mu\text{m}$ ) single laser pulse ( $\sim 250 \text{ ps}$  full width at half-maximum) interacting with a massive planar metallic target (with relatively high  $Z$ ) using the focal plane positioned inside of the target could produce plasma jets with very interesting parameters [7, 8]. For formation of a convergent narrow jet an annular structure of the focal spot proved to be indispensable [9]. It should be pointed out that the annular target irradiation is created spontaneously during the laser beam – plasma interaction from an initially flat laser radiation distribution providing that the focal point of a focusing lens is situated inside the target. In Fig. 1a,b shadowgraphic and interferometric images of a typical Cu plasma jet for a laser energy of 70 J at different instants of its evolution are presented. The plasma jet creation starts about 2 ns after the laser action. At this time the emitted plasma reaches a relatively high

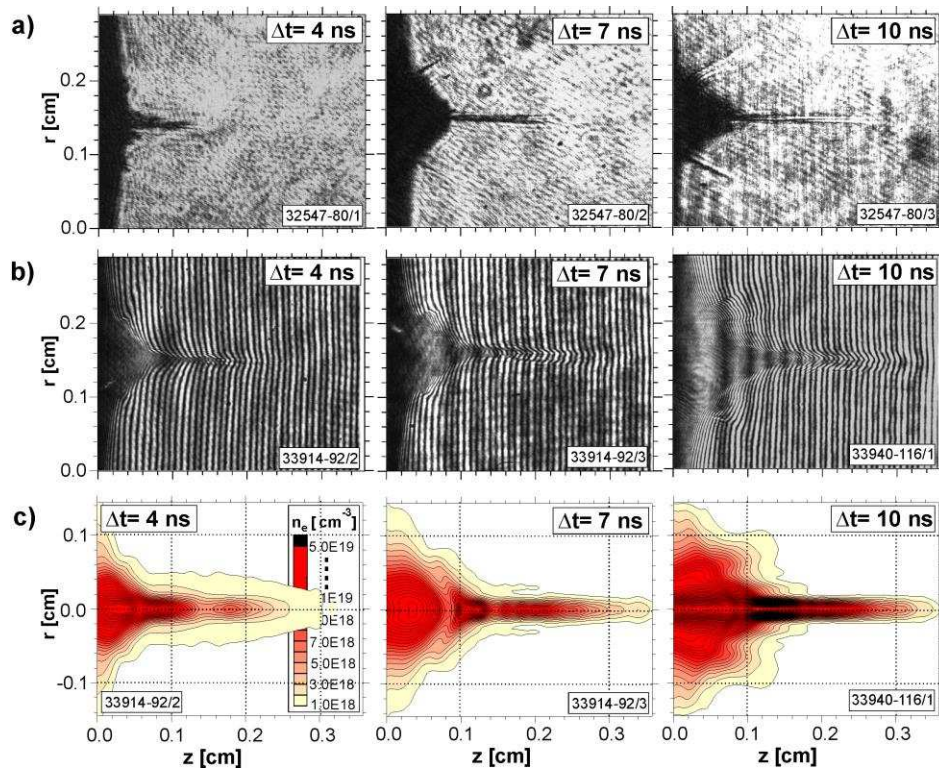


Fig. 1. Illustration of the typical plasma jet generated by the action of laser beam on the Cu planar target: a – shadowgrams, b – interferograms, and c – electron equidensitograms.

density. Due to the annular target irradiation a part of the plasma expands towards the axis to collide itself there creating an elongated thin plasma configuration. Since the radial component of the plasma velocity decreases with a growing distance from the target the plasma collision is obviously more effective closer to the target. The region of the strong plasma collision is seen on the shadowgrams in a form of a thin line, the length of which grows in time so as to stop after about 8-10 ns. This region on the interferograms corresponds to a sharp form of interferometric fringes at the axis. The farther region (unseen on the shadowgrams) with smooth interferometric fringes at the axis corresponds to the zone of weak plasma collision. In Fig. 1c the electron equidensitograms corresponding to the above interferograms are drawn. The jets produced by this method have the following parameters: maximum length  $\sim 4$  mm (without the plasma jet pedestal), radius  $\sim 300$   $\mu\text{m}$ , velocity up to  $7 \times 10^7$  cm/s, and electron density above  $10^{19}$   $\text{cm}^{-3}$ .

### 3. Disk impact method of plasma jet generation

To realize this plasma jet generation method in the experiment our attention was focused on the flyer disk impact effects observed in a long period after the collision occurred, i.e. up to about 23 ns after the laser action (17 ns after the impact). It required to employ a

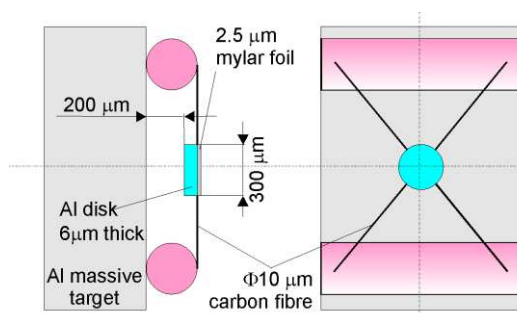


Fig. 2 Double target construction.

special target construction which made it possible to visualize the plasma generation and subsequent expansion across the whole massive target surface (see Fig. 2). The laser provided a 250 ps (FWHM) pulse with the energy of 130 J at the first harmonic ( $\lambda_1=1.315$   $\mu\text{m}$ ). The sequences of subsequent electron equidensitograms and spatial distributions of the electron density in Fig. 3 show the evolution of the disk-produced plasma. The plasma as a whole consists of two parts:

(i) the axial stream with the radius of about  $250\ \mu\text{m}$  and (ii) the lateral plasma, of the radius of above  $1.5\ \text{mm}$ . To reach the distance  $1.5\ \text{mm}$  the lateral plasma had to start earlier than the axial one. It is connected with that the lateral plasma originates from the disk edge where the plasma outflow is not limited, whereas the axial component can expand only after the disk disappears. The electron density of the lateral plasma exceeds  $10^{19}\ \text{cm}^{-3}$ , thus at the beginning of the post-impact stage the participation of this plasma as a whole reaches 90 %. At later time the role of the axial plasma should grow and one can suppose that in due time the axial plasma will dominate.

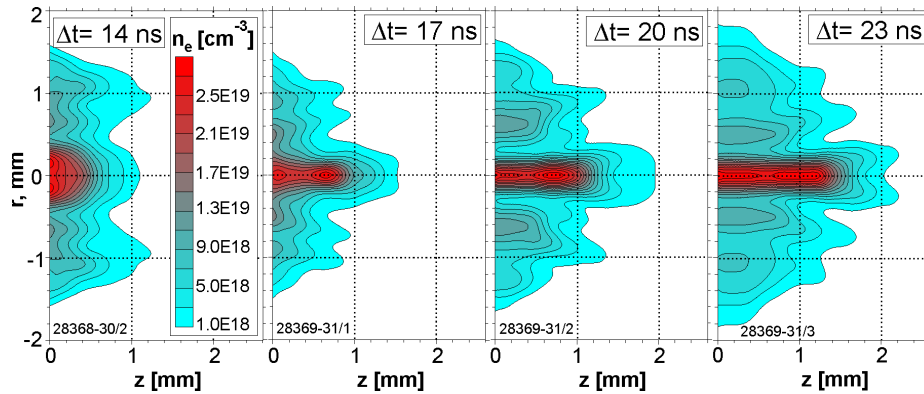


Fig. 3 The sequence of electron density distributions.

Velocities of the axial plasma streams (determined at relatively high density levels of  $n_e > 10^{19}\ \text{cm}^{-3}$ ) are reaching  $10^7\ \text{cm/s}$ . The maximum electron density in the plasma stream is close to  $3 \cdot 10^{19}\ \text{cm}^{-3}$ . A more detailed description of this method can be found in Ref. 10.

#### 4. Cumulatively produced jet

The experiment was inspired by the theoretical and numerical analyses presented in Ref. 11. Investigations were performed with the use of the first harmonic of the PALS iodine laser radiation at the energy of about  $550\ \text{J}$ . The cones made of Al foil with thicknesses of  $9\ \mu\text{m}$  had the apex angle of  $90^\circ$  and the height  $H=250\ \mu\text{m}$ . The target construction and the cross-section photograph of an exemplary Al cone are shown in Fig. 4.

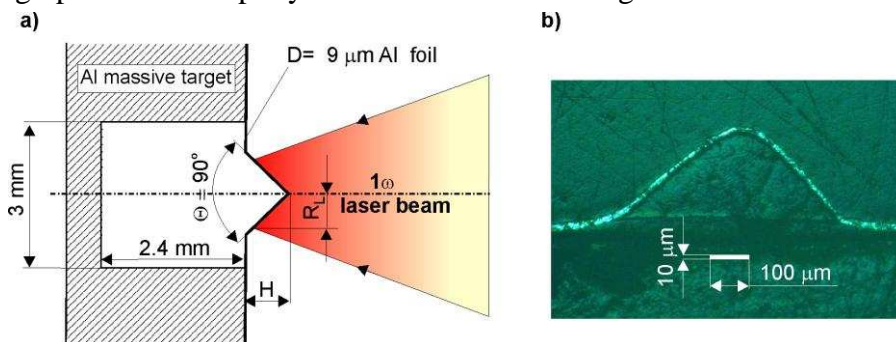


Fig. 4 The target construction (a) and the cross-section photograph of the exemplary Al cone (b).

One can estimate that the actual thickness of the cone wall is smaller by about 30% than the initial foil thickness. The focal spot radius,  $R_L$ , was decreased step by step by  $50\ \mu\text{m}$  from  $250\ \mu\text{m}$  to  $100\ \mu\text{m}$ . It allowed us to get different intensities of the laser radiation at the cones lateral surface. Although in our experiment we started from  $R_L=250\ \mu\text{m}$ , satisfactory results were obtained just for  $R_L=100\ \mu\text{m}$ . So, these results are demonstrated here. The sequences of electron equidensitograms of the cumulatively produced plasma jets are presented in Fig. 5. One can see that after  $1\ \text{ns}$  the cumulative jet reaches a distance from the foil surface of about  $0.7\ \text{mm}$ . Taking into consideration the  $0.2\ \text{mm}$  plasma way inside the cone, the plasma jet velocity at the first nanosecond was estimated to be higher than  $0.8 \times 10^8\ \text{cm/s}$ . However, that

high plasma velocity lasts for a very short time, decreasing very fast below  $0.4 \times 10^8$  cm/s after next 3 ns. The plasma jet is characterized by a relatively high electron density, considerably above  $10^{19}$  cm<sup>-3</sup>, with a steep plasma jet front at the initial stage of the jet propagation.

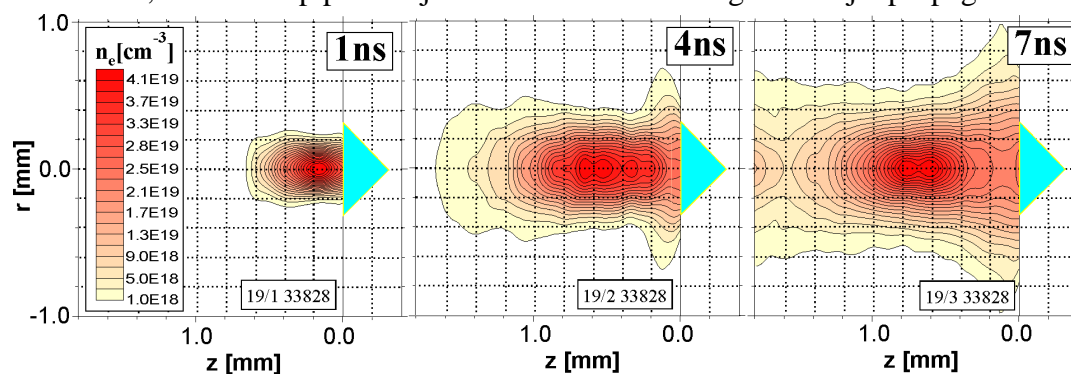


Fig. 5 Sequence of the electron equidensitograms corresponding to propagation of the cumulative jet.

## 5. Conclusions

Our investigations have shown that there is a possibility to create plasma jet with parameters very promising in the astrophysical context and for inertial confinement fusion by means of very simple methods. Of course, the jet parameters achieved in our experiments are not completely satisfactory, particularly in the case of the indirect methods, for which professional technologies of the targets prefabrication are necessary. However, the reported experiments constitute the first step on the way to the best jets.

**Acknowledgement:** The work was supported in part by the Association EURATOM-IPPLM (contract No FU06-CT-2004-00081), by the Ministry of Schools, Youth and Sports of the Czech Republic (project No LC528), by the Access to Research Infrastructures activity in the 6FP of the EU (contract RII3-CT-2003-506350, Laserlab Europe), and by the IAEA Research Contract No. 13781 as well as the IPPLM contribution to the HiPER project.

## References:

1. B. A. Remington, R. P. Drake, and D. D. Ryutov, *Rev. Mod. Phys.* 78, 755 (2006).
2. S. V. Lebedev, J. P. Chittenden, F. N. Beg, S. N. Bland, A. Ciardi, D. Ampleford, S. Hughes, M. G. Haines, A. Frank, E. G. Blackman, and T. Gardier, *Astroph. Journ.* 562, 113 (2002).
3. S. R. Goldman, S. E. Caldwell, M. D. Wilke, D. C. Wilson, Cris W. Barnes, W. W. Hsing, N. D. Delamater, G. T. Schappert, J. W. Grove, E. L. Lindman, J. M. Wallance, and R. P. Weaver, *Physics of Plasmas* 6, 3327 (1999).
4. E. Blue, S. V. Weber, S. G. Glendinning, N. E. Lanier, D. T. Woods, M. J. Bono, S. N. Dixit, C. A. Haynam, J. P. Holder, D. H. Kalantar, B. J. MacGowan, A. J. Nikitin, V. V. Rekow, B. M. Van Wonterghem, E. I. Moses, P. E. Stry, B. H. Wilde, W. W. Hsing, and H. F. Robey, *Phys. Rev. Letters PRL* 94, 095005 (2005).
5. D. R. Farley, K. G. Estabrook, S. G. Glendinning, S. H. Glenzer, B. A. Remington, K. Shigemori, J. M. Stone, R. J. Wallance, G. B. Zimmerman, and J. A. Harte, *Phys. Rev. Lett.* 83, 1982 (1999).
6. K. Shigemori, R. Kodama, D. R. Farley, T. Koaste, K. G. Estabrook, B. A. Remington, D. D. Ryutov, Y. Ochi, H. Azechi, J. Stone, and N. Turner, *Phys. Review E* 62, 8838 (2000).
7. A. Kasperczuk, T. Pisarczyk, S. Borodziuk, J. Ullschmied, E. Krousky, K. Masek, K. Rohlena, J. Skala and H. Hora, *Physics of Plasmas* 13, 062704-1 (2006).
8. A. Kasperczuk, T. Pisarczyk, S. Borodziuk, J. Ullschmied, E. Krousky, K. Masek, M. Pfeifer, K. Rohlena, J. Skala and P. Pisarczyk, *Physics of Plasmas* 14, 032701-1 (2007).
9. A. Kasperczuk, T. Pisarczyk, J. Badziak, R. Miklaszewski, P. Parys, M. Rosinski, J. Wolowski, Ch. Stenz, J. Ullschmied, E. Krousky, K. Masek, M. Pfeifer, K. Rohlena, J. Skala, and P. Pisarczyk, *Physics of Plasmas* 14, 102706-1 (2007).
10. A. Kasperczuk, T. Pisarczyk, S. Borodziuk, S. Yu. Gus'kov, J. Ullschmied, E. Krousky, K. Masek, M. Pfeifer, K. Rohlena, J. Skala, M. Kalal, J. Limpouch and P. Pisarczyk, *Optica Applicata* 37, 141-152 (2007).
11. P. Velarde, F. Ogando, S. Eliezer, J.M. Martinez-Val, J.M. Perlado, and M. Murakami, *Laser Part. Beams* 23, 43 (2005).